Cavitation of some copper alloys for naval propellers: electrolyte effect

Cavitation of some copper alloys for naval propellers: electrolyte effect

M V Biezma Moraleda[1], L Merino Galván[1], P Linhardt[2]

[1]Dpto. de Ciencia e Ingeniería del Terreno y de los Materiales,
Universidad de Cantabria, Dique de Gamazo 1, 39004 Santander, Spain
[2]Institute for Chemical Technologies and Analytics, Technische Universität Wien,
Getreidemarkt 9, 1060 Vienna, Austria

biezmav@unican.es

Abstract. Efficient shipping is becoming more challenging, not only because of the increasing demand for this means of transport, the performance requirements and the optimisation of resources, but also because of the environmental constraints. Cavitation is a harmful phenomenon that can affect different systems of a ship such as pumps, valves, impellers, pipes, etc., but is particularly known for its effect on propellers, associated with loss of power and even impairment of structural integrity. The mechanical effect of cavitation on metallic materials is in general superimposed by corrosion and may thus lead to a synergistic degradation phenomenon. In this work, the cavitation behaviour and the potential synergistic effect with corrosion was evaluated for three widely used copper-based alloys, NAB (Nickel Aluminium Bronze), MAB (Manganese Aluminium Bronze), and a brass (low lead content) using three types of water: natural seawater, synthetic seawater and synthetic brackish water. Experiments were carried out in an ultrasonic bath, followed by structural surface characterisation. The main result is that MAB is most susceptible to both, general surface damage and deep localized attack. This is attributed to its poor ability in regenerating the protective layer, the area ratio of their phases and the high hardness of the κ-phase, in combination with high mechanical stresses during impacts affecting the grain boundaries. Moreover, natural seawater was found to increase cavitation, attributable to the dispersion of micro-particles, while brackish water with its content of sulfidic species was found to promote the strongest synergy between corrosion and cavitation.

1. Introduction

The phenomenon of cavitation, i. e. the growth and collapse of vapor bubbles in a liquid due to local pressure fluctuations, has been and still is extensively studied within the field of marine engineering. One of its undesired consequences are the mechanical impacts on solid surfaces which arise from the collapsing bubbles, possibly leading to damages at components. The attempt to achieve greater efficiency of systems and navigation, resulting in the design of larger propellers operating at higher revolutions, increases the likelihood of cavitation and in combination with the corrosive environment the potential for damages due to this phenomenon has increased [1]. In particular, considering the need to extend the service life of propellers, to save material and manufacturing costs, to extend the operating regime, etc., an exhaustive study of cavitation is required for design optimization [2],[3],[4]. Moreover, environmental conditions must be taken into account, as they can cause corrosion problems and aggravate the phenomenon of cavitation, while, on the other hand, cavitation may also accelerate

the corrosion processes. This appears critical in marine conditions due to the hostile environment of rather complex chemical composition, possibly aggravated by the presence of contaminants [5, 6].

In this study, the cavitation behaviour of three copper alloys (nickel-aluminium bronze, manganese-aluminium bronze, and a duplex brass) as are used for naval propellers, were investigated with respect to the interaction with different electrolytes, i.e. different water compositions: artificial seawater, artificial brackish water, and natural seawater.

2. Experimental

2.1. Materials

Alloys most commonly used for propellers, impellers and valves due to their good mechanical properties and corrosion resistance were studied in their as-cast state: manganese aluminium bronze (MAB), nickel aluminium bronze (NAB), and a brass (CB773S). The brass may be considered an *ecobrass*, having a low Pb content and appearing attractive in view of future environmental restrictions. The chemical composition of the materials was provided by the suppliers and is summarized in Table 1. Their hardness was assed previously [7] by 205 HB (NAB), 207 HB (MAB), and 158 HB for the brass.

Table 1. Chemical composition of the alloys (%wt).

Alloy	Cu	Al	Ni	Fe	Mn	Zn	Pb	Sn	Si
NAB	79.80	9.31	4.57	4.92	1.23	0.0492	0.0056	0.0058	0.0393
MAB	70.9	7.12	2.06	4.59	12.63	2.35	0.0126	0.0059	0.0345
CB773S	57.97	0.17	0.01	0.15	-	≈ 40	0.09	0.03	-

The specimens were machined to 20 x 15 mm with one corner rounded by a radius of ca. 13 mm. The thickness of these coupons was 3 mm. In view of a desired surface roughness for propellers of 0.6 µm, the specimens received a surface finish by grinding with SiC paper up to # 1200 and final polishing with diamond paste from 6 down to 0.25 µm.

The microstructures of the materials as observed after polishing are presented in figure 1. NAB consists of α phase, β phase and four rather small κ-phases (formed by Fe3Al and NiAl, ca. 5 µm). MAB is a bronze that consists of α-phase (rich in copper), β-phase and relatively large κ-phases (mainly rich in Fe, Mn, ca. 40 µm wide) [8]. The brass exhibits a duplex structure consisting of α- (rich in copper) and β-phase (rich in zinc).

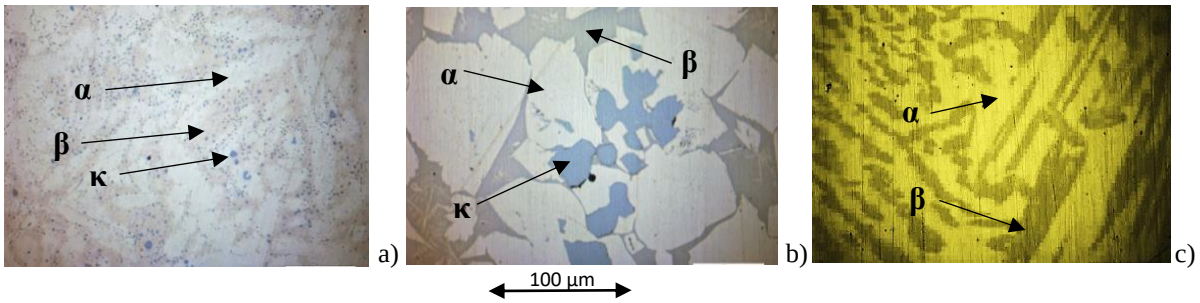

Figure 1. Microstructures of tested materials. a) MAB, b) NAB, c) brass.

2.2. Test media

Three test media were selected to reflect different waters that propellers may exposed to during service conditions. Consequently, they also represent the electrolytes, which are relevant for the electrochemical corrosion processes, which act on the metals in general, and which get modified by cavitation.

Artificial Seawater (ASW) and Artificial Brackish Water (ABW) were prepared by dissolving the relevant salts in deionized water, based on a standard [9]. Table 2 presents their composition. Santander Bay Water (SBW) was collected in the Bay of Santander, Spain, and its typical physicochemical characteristics, as provided by the Instituto Oceanográfico de Santander, are listed in Table 3.

Table 2. Salts used for preparing 1 L of ASW and ABW.

Chemical compounds	ASW	ABW
sodium chloride, 28.0 g NaCl	X	X
magnesium chloride, 5.0 g $MgCl_2 \cdot 6\ H_2O$	X	X
calcium chloride, 2.4 g $CaCl_2 \cdot 6\ H_2O$	X	X
magnesium sulphate, 7.0 g $MgSO_4 \cdot 7\ H_2O$	X	X
sodium bicarbonate, 0.20 g $NaHCO_3$	X	-
tri-sodiumcitrate, 1.0 g $C_6H_5Na_3O_7 \cdot 2\ H_2O$	-	X
thioacetamide, 0.50 g CH_3CSNH_2.	-	X

Table 3. Physicochemical properties of SBW.

Parameter	Quantity
Density	1.025 g/mL
pH	8.2
Acidity	0.06-0.18 mEq/L
Alkalinity	2.36-2.72 mEq/L
Hardness	6.4-6.8 g $CaCO_3$/L
Ammonium	0-50 µg N-NH_4^+/L
Calcium	320-680 mg Ca/L
Nitrite	0-25 µg N-NO_2^-/L
Nitrate	100-125 mg N-NO_3^-/L
Sulphate	720-900 mg S- SO_4^{2-}/L
Phosphate	0-23 g P-PO_4^{3-}/L
Chloride	17.6-19.2 g Cl^-/L

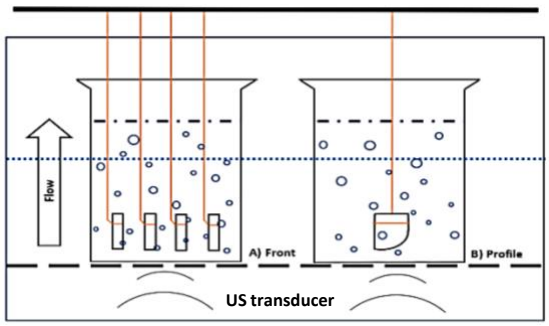

Figure 2. Position of specimens vertically inside beakers in the ultrasonic bath.

2.3. Cavitation testing

An Emerson Branson 2800 ultrasonic bath, operating at 40 kHz at a power of 100 W and filled with tap water was used to perform the cavitation tests. The test media were filled in beaker glasses placed in the bath and the specimens were introduced vertically by hanging them in, ca. 0.5 mm above the bottom. figure 2 provides a schematic view of the test setup.

The test time was 45 min. or 90 min. (in two intervals of 45 min. each), allowing to observe the surface changes in the early stage, and at some more severe state of destruction. The temperature in the bath was kept below 30 °C during testing. All tests were done in triplicate at minimum.

2.4. Evaluation of tested specimens

To observe type and level of cavitation damage and for finding a correlation with the microstructural features, the tested specimens were investigated using a Leica EZ4 HD stereo microscope and a Leica DM 4000 - U optical microscope.

For quantification of the damage, each side of the specimen was subdivided by a mesh (40x40) and each surface element was evaluated by 0 (no damage) and 1 (damage found), yielding a value for the Affected Zone as the percentage of damaged surface elements (% AZ). Moreover, the mean pit diameter (Φm, µm) was calculated by averaging the diameter of the pits in different areas. It should be noted that weight loss has not been considered for evaluation since the amount of material loss during the tests was found insufficient for this method.

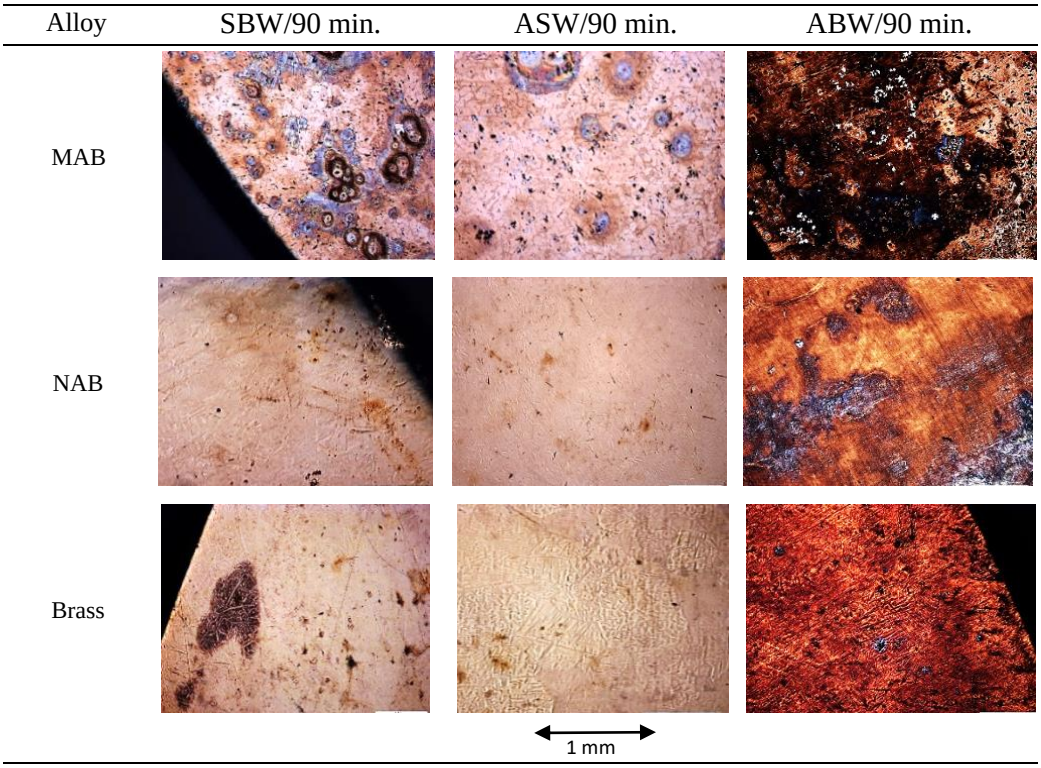

Figure 3. Surface views of specimens after 90 min. testing.

3. Results

Figure 3 presents views on the surface of tested specimens after 90 min. of testing and Table 4 summarizes the results of cavitation damage evaluation after 45 min and 90 min test time in SBW and ASW. For ABW, this method of quantification was not successful since a well adhering crust of

corrosion products prevented from assessing the data accurately This may be anticipated by figure 3 and particularly for MAB in figure 4 at larger scale, comparing the effect of the three test media.

Table 4. Affected zone (AZ) and mean pitting diameter (Φ_m) for MAB, NAB and brass in SBW and ASW.

	AZ (%)						Φ_m (µm)					
	45 min			90 min			45 min			90 min		
	MAB	NAB	Brass	MAB	NAB	Brass	MAB	NAB	Brass	MAB	NAB	Brass
SBW	46	24	28	82	39	47	45	10	15	90	24	40
ASW	35	15	15	57	24	26	25	3	7	48	12	16

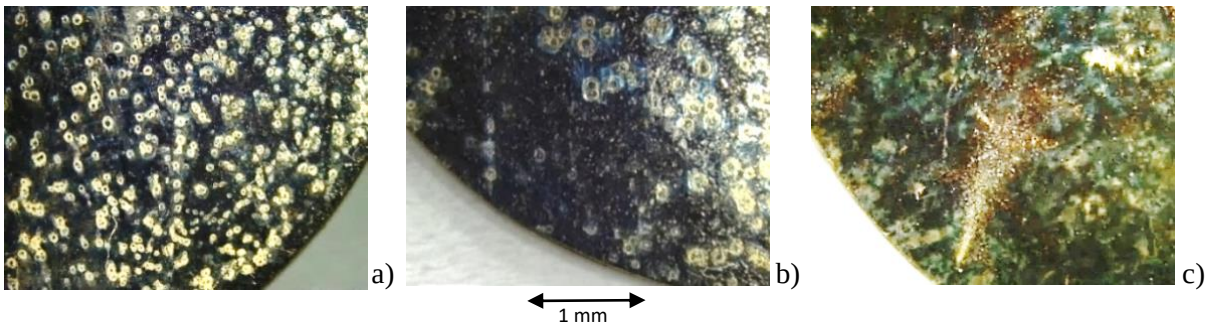

Figure 4. MAB tested for 90 min. in a) SBW, b) ASW, c) ABW.

The data in Table 4 indicate that the damage increases with time for both parameters, density of damage (AZ) and size of damaged spots (Φm). There appears a systematic ranking for the susceptibility of the materials to cavitation damage in this test: MAB>brass>NAB, which is more pronounced for Φm than for AZ. E.g. we find for ASW after 90 minutes for Φm 48:12 µm (MAB:NAB) and for AZ 57:24 % (MAB:NAB), and similar ratios were gained with SBW. However, damage parameter values for SBW appear significantly higher (about double) than those for ASW.

For the microscopic inspection of the surfaces, the specimens tested for 45 min. were found more suitable since the degree of damage was sufficiently low to reveal the consequences of impacts on the different materials. Figure 5 presents typical observations made with ASW tested specimens. For brass and NAB, mainly effects of plastic deformation from the cavitation impacts were observed, with more diffuse appearance (brass) up to distinct impact craters (NAB). For MAB, however, damages appeared preferentially as deep pits related to locations where the kappa phase is present, which was removed in part (attack at the boundary to surrounding alpha), and sometimes it erodes completely, leaving some kind of brownish halo, presumably a thin layer of corrosion products, on the surrounding surface.

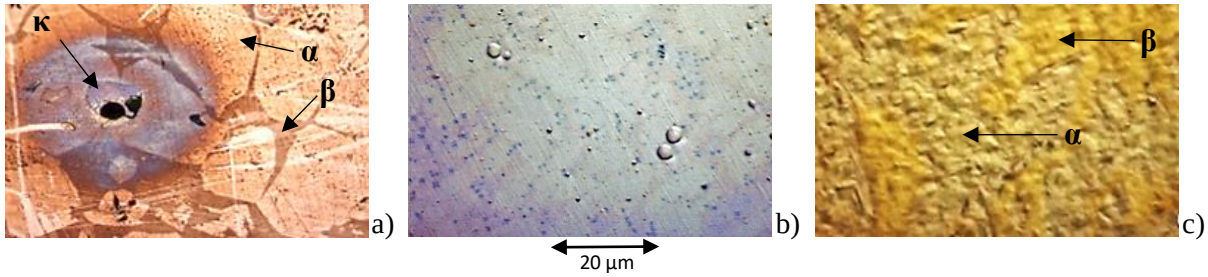

Figure 5. Typical surface damage phenomena at a) MAB, b) NAB, and c) brass, tested in ASW.

With SBW, the phenomena were similar to those observed with ASW but there were indications for the impacts having been more severe: figure 6a presents an example from brass, where some material appears eroded in an irregular manner, affecting mainly the alpha phase. figure 6b provides an example from NAB, where rather deep pits have appeared, accompanied by massive brown halos. Their relation to a certain microstructural feature is not traceable any more, but the color of the halo indicates the presence of iron and thus indicates the dissolution of some kappa phase, mainly those with higher content of this chemical element, denominated κ_I and κ_{II}.

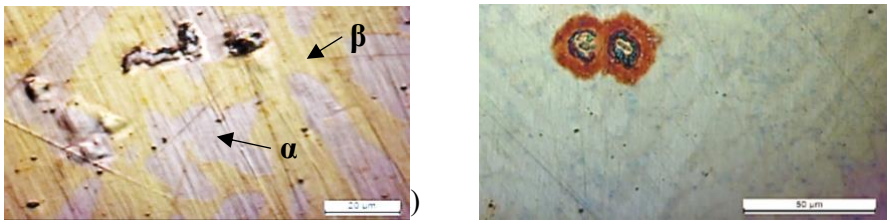

Figure 6. Typical surface damage phenomena at a) brass and b) NAB, tested in SBW.

With ABW it was generally hard to identify distinct locations of damage due to the accumulated corrosion products (figure 3) being darker for MAB in relation to NAB and brass. After their careful removal, the surface features summarized in figure 7 could be observed. The attack at MAB (figure 7a) occurred preferentially at the interface between κ- and α-phase, or by complete removal of κ, accompanied by intense halos of corrosion products, indicating a significant contribution of corrosion to the removal of material. This phenomenon is similar that observed with ASW. With NAB (figure 7b), preferential localized removal of β-phase was observed, leading to a dendritic spreading of the material loss by corrosion, emerging from impact sites. A similar pattern was found for brass (figure 7c), where also the β-phase gets preferentially removed in a very localized manner.

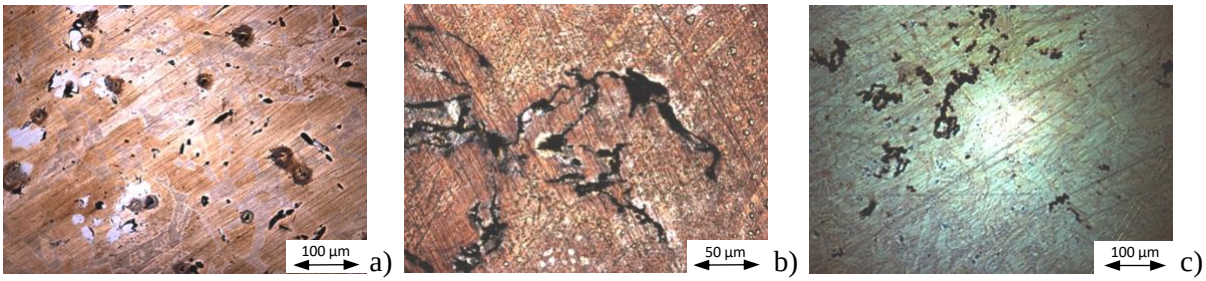

Figure 7. Typical surface damage phenomena at a) MAB, b) NAB, and c) brass, tested in ABW.

4. Discussion

The data in Table 4 and the impressions from microscopic inspection (figures 3, 5, and 6) indicate natural seawater, i.e. SBW, acting more aggressive on the tested materials under cavitation conditions compared to the synthetic medium (ASW). However, this increased aggressiveness appears not related to corrosiveness (the appearance of corrosion products is rather limited in both media), but rather to more frequent and more intense impacts from cavitation occurring in SBW. This may be explained by the suspended solids which are present in natural waters and which modify substantially the cavitation behavior of the water. As reported previously [10], these microscopic particles may serve as nucleation sites for the cavitation-caused vapor bubbles, increasing the probability of cavitation impacts.

Under cavitation conditions, surface inhomogeneity may induce the formation of pits, as was observed on MAB and NAB. A particular role in this context play the κ-phases, i.e. intermetallic compounds rich in Fe, Al and Ni, and this observation is in agreement with results from previous studies [11, 12]. κ-phases of MAB and NAB are different in chemical composition, size, shape and

distribution and may induce the nucleation of bubble implosion, driving their erosion due to large dislocations between grain boundaries [13], in particular at the α/κ-interface. Such a surface inhomogeneity induces a continued erosion process since it acts as preferential site for bubble implosions causing an accumulative effect of damage. Consequently, the material is unable to recover its protective layer, enhancing the synergistic interaction between cavitation and corrosion [14]. Besides, the turbulent flow conditions under cavitation conditions enhance the mass transport of oxidant and aggressive species to the metal surface by eliminating diffusion limitation, thus accelerating the corrosion processes [11].

By contrast, brass suffers mainly plastic deformation affecting preferentially the α-phase, which contains less Zn than the β-phase and therefore is less hard [15].

ABW turned out to create a strong additional corrosive effect to the mechanical cavitation damaging. This may be related to its content of sulfidic species, which is well known to act detrimental on copper and its alloys by retarding the formation of the regular, copper oxide-based protective layer [2, 16]. Moreover, the corrosion products on the surface may have influenced the further nucleation of impacts, resulting in a significant change in the damaging pattern, particularly for NAB and brass (Figure 7b, c).

To summarize, a significant effect of the composition of the test medium on cavitation damage was observed. Natural seawater and synthetic seawater, although of very similar chemical composition, were found to induce different degrees of cavitation damage, attributed to some dispersed solid phase in the natural water. On the other hand, artificial brackish water was found to add a substantial contribution of corrosion to the cavitation process. Its contribution is related to the presence of dissolved sulfidic species, which negatively affects the ability of the material to develop a new protective layer after an impact event.

5. Conclusions

Cavitation corrosion is a rather complex phenomenon: cavitation, as a mechanical phenomenon, erodes the most brittle and hard phases of the material, which are frequently the intermetallic compounds. Corrosion, as an electrochemical phenomenon, attacks the most reactive phases and controls the formation of a more or less protective layer, depending on the chemical composition of the electrolyte. A continuous cavitation process removes corrosion products and impacts until the brittle phases are eliminated.

There appears a systematic ranking for the susceptibility of the investigated materials to cavitation damage in this test, independent of the test medium: MAB>brass>NAB. This behaviour is attributable to the chemical composition, distribution and particular large size of the rather hard and more brittle κ-phase of MAB that acts as nucleation site for impact from bubble collapse.

Artificial brackish water, ABW, is the most aggressive test medium, causing a strong corrosion contribution to the cavitation effect. This is attributed to the presence of sulfidic species which reacts with copper to non-protective corrosion products.

Natural sea water, SBW, was found to act more aggressive under cavitation conditions compared to the synthetic medium, ASW. This may be explained by the suspended solids present in the natural water as these microscopic particles may serve as nucleation sites during the cavitation process.

Acknowledgement: to JC Navalips, Maliaño, Spain, and Latones del Carrión, Córdoba, Spain, for providing bronzes and brass, respectively, and to Gobierno de Cantabria, for financial support of project SUBVTC-2021-0024.

References

[1] Ivan Richardson 2016 Guide to Nickel Aluminium Bronze for Engineers (ed. Carol Powell), *Copper Development Association Publication No 222*, Copper Development Association
[2] Zhao X, Qi. Y, Wang J, Peng TX, Zhang Z, Li K 2020 *Metals* **10** 1227
[3] Doijode P S, Hickel S, van Terwisga T, Visser K 2022 *Applied Ocean Research* **124** 103174

[4] Peters A, Lantermann U, Moctar O 2018 *Wear* **408–409** 1–12
[5] De Sanchez S R, Schiffrin D . 1982 *Corrosion Science* **22** 585-607
[6] Song Q N, Xu N, Bao Y F, Jiang Y F, Gu W, Zheng Y, Qiao Y X 2017 *Acta Metall. Sin.* (Engl. Lett.) **30** 712–720
[7] Cobo I, Biezma M V, Linhardt P 2022 *Mater. Corr.* **73** 1788-1799
[8] Mota N M, Tavares S S M, Nascimento A, Zeeman G, Biezma-Moraleda M V 2021 *Eng. Failure Analysis* **129** 105732
[9] DIN 50905-4 2018 Deutsches Institut für Normung e. V. (Beuth Verlag GmbH, Berlin, Germany)
[10] Kunpeng S, Jianhua W, Dingkang X 2020 *Ultrason Sonochem* **68** 105214
[11] Biezma M V, Linhardt P 2022 *11th Iberian Conference on Tribology 6-7 October 2022 – Setúbal, Portugal, Book of Abstracts* 96-98
[12] Linhardt P, Kührer S, Ball G, Biezma M V 2018 *Mater. Corros.* **69** 358-364
[13] Karimi A, Martin J L 1986 *International Metals Reviews* **31** 1–26
[14] Linhardt P, Biezma, M V, Strobl S, Haubner R 2023 *Solid State Phenomena* **341** 25-30
[15] Moriarty M, Wu Y, Murray T, Hutchinson C 2021 *Corros. Sci.* **184** 109366
[16] Schüssler A, Exner H E 1993 *Corros. Sci.* 34 1793-1802